International Journal of Pharmaceutics 364 (2008) 94–101

Contents lists available at ScienceDirect

International Journal of Pharmaceutics

journal homepage: www.elsevier.com/locate/ijpharm

Pharmaceutical Nanotechnology

Amine-functionalized gold nanoparticles as non-cytotoxic and efficient intracellular siRNA delivery carriers

Soo Hyeon Lee, Ki Hyun Bae, Sun Hwa Kim, Kyu Ri Lee, Tae Gwan Park*

Department of Biological Sciences, Korea Advanced Institute of Science and Technology, Daejeon 305-701, South Korea

ARTICLE INFO

Article history:
Received 25 April 2008
Received in revised form 4 July 2008
Accepted 27 July 2008
Available online 3 August 2008

Keywords:
Gold nanoparticles
Small interfering RNA (siRNA)
Poly(ethylene glycol)
Polyelectrolyte complex
Gene delivery

ABSTRACT

Gold nanoparticles chemically modified with primary amine groups were developed as intracellular delivery vehicles for therapeutic small interfering RNA (siRNA). The positively charged gold nanoparticles could form stable polyelectrolyte complexes through electrostatic interactions with negatively charged siRNA–polyethylene glycol (PEG) conjugates having a cleavable di-sulfide linkage under reductive cytosol condition. The resultant core/shell type polyelectrolyte complexes surrounded by a protective PEG shell layer had a well-dispersed nanostructure with a hydrodynamic diameter of 96.3 ± 25.9 nm, as determined by dynamic light scattering and transmission electron microscopy. Confocal laser scanning microscopy revealed that the nanosized polyelectrolyte complexes were efficiently internalized in human prostate carcinoma cells, and thus enhanced intracellular uptake of siRNA. Furthermore, the siRNA/gold complexes significantly inhibited the expression of a target gene within the cells without showing severe cytotoxicity. The current study demonstrated that positively charged gold nanoparticles could be potentially applied for intracellular delivery of siRNA.

1. Introduction

Small interfering RNAs (siRNAs) have recently emerged as a promising nucleic acid agent for treating various diseases such as cancer, because of their superior ability to silence target genes in a specific manner. It has been demonstrated that siRNA induces sequence-specific degradation of complementary mRNA, leading to knock down of a target protein in post-transcriptional level (Dorsett and Tuschl, 2004; Novina and Sharp, 2004). Nevertheless, the use of siRNA in clinical applications has been questioned due to several obstacles including poor intracellular uptake and severe enzymatic degradation under in vivo circumstances (Dykxhoorn and Lieberman, 2005; Ryther et al., 2005). To overcome the limitations, various cationic polymers, peptides, and lipids have been extensively utilized to form nanosized polyelectrolyte complexes via electrostatic interactions with siRNA. These polyelectrolyte complexes could protect siRNA from degradation by nucleases and facilitate cellular uptake of siRNA into target cells or tissues by an endocytic pathway (Schiffelers et al., 2004; Hassani et al., 2005; Park et al., 2006). However, there are still serious problems such as cytotoxicities induced by cationic carriers and low stability of the complexes in the presence of serum.

Gold nanoparticles have attracted increasing attention in a variety of biomedical fields including DNA mismatch detection, biomolecular sensing, and hyperthermal cancer therapy due to their unique and controllable optical properties termed surface plasmon resonance (Storhoff et al., 1998; Otsuka et al., 2001; Hirsch et al., 2003). Recently, many attempts have been made to utilize gold nanoparticles as intracellular gene carriers because they have several advantages of straightforward synthesis, easy modification of surfaces with thiolated molecules, and biocompatibility with cells or tissues. For example, thiol-modified antisense oligonucleotides were directly conjugated onto gold nanoparticles for regulation of protein expression in cells (Rosi et al., 2006). Gold nanoparticles chemically modified with primary and quaternary amine moieties were ionically interacted with plasmid DNA, and they exhibited more efficient intracellular delivery than the conventional transfection agents (Sandhu et al., 2002; Niidome et al., 2004). Furthermore, it was suggested that gold nanoparticles could be functionalized with various antibodies, peptides, and small molecular ligands to achieve a target cell-specific uptake, endosome escape, and nuclear localization for efficient gene delivery.

In this study, we demonstrated the use of amine-functionalized gold nanoparticles for intracellular siRNA delivery. Green fluorescence protein (GFP) siRNA was conjugated to polyethylene glycol (PEG) via a di-sulfide linkage that can be cleaved to allow release of an intact siRNA under a reductive environment in the cyto-

* Corresponding author. Tel.: +82 42 869 2661; fax: +82 42 869 2610.
E-mail address: tgpark@kaist.ac.kr (T.G. Park).

0378-5173/$ – see front matter © 2008 Elsevier B.V. All rights reserved.
doi:10.1016/j.ijpharm.2008.07.027

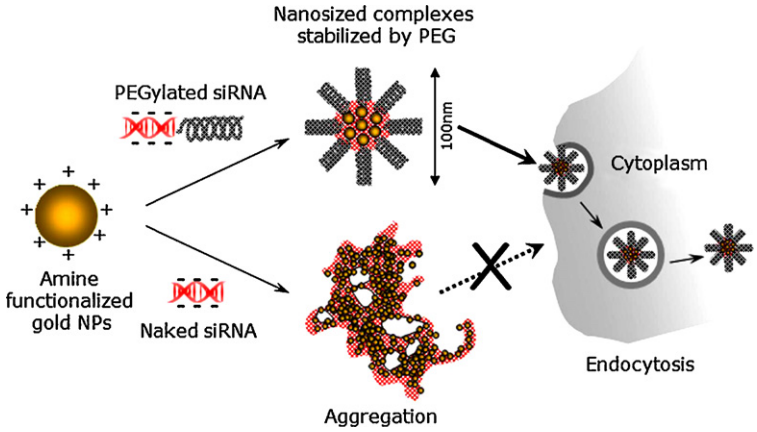

Scheme 1. Schematic illustration for polyelectrolyte complexes formed from amine-functionalized gold nanoparticles (AF-AuNPs) with siRNA and siRNA–PEG conjugate.

plasm. We have previously shown that siRNA–PEG conjugates were complexed with cationic polymers, peptides, and lipids to produce polyelectroyte complex micelles. The cationic species interact with the anionic siRNA part via ionic interactions to form a charge-neutralized inner core, while the PEG part in the conjugate was oriented outside to generate a PEG shell layer. The resultant micelles exhibited a greater level of gene inhibition compared to the naked siRNA (Kim et al., 2006; Lee et al., 2007). Here, we used cationic and biocompatible gold nanoparticles as a core-condensing agent to produce nanosized polyelectrolyte complexes capable of efficiently delivering siRNA into cells. It was hypothesized that cationic gold nanoparticles of ~15 nm could interact with siRNA–PEG conjugates to form sterically stabilized siRNA/gold nano-complexes suitable for intracellular delivery. We investigated the structure and dispersion stability of the siRNA–PEG/gold polyelectrolyte complexes by dynamic light scattering (DLS) and transmission electron microscopy (TEM). The extent of intracellular uptake and GFP gene silencing effect were evaluated to explore the potential of the amine-functionalized gold nanoparticles as intracellular siRNA carriers.

2. Materials and methods

2.1. Materials

Methoxy-poly(ethylene glycol) terminally functionalized with a thiol group (mPEG–SH, M_w = 5000) was obtained from Sunbio (Anyang, Korea). Branched polyethylenimine (PEI, M_w = 25,000), chloroauric acid ($HAuCl_4$), sodium borohydride ($NaBH_4$), cysteamine dihydrochloride, and 4′,6-diamidino-2-phenylindole (DAPI) were purchased from Sigma Chemical Co. (St. Louis, MO). Lipofectamine2000™ and LysoTracker Green DND-99 were purchased from Invitrogen (Carlsbad, CA) and Molecular Probes (Eugene, OR), respectively. Cell counting kit-8 (CCK-8) was obtained from Dojindo (Kumamoto, Japan). Micro-BCA protein assay kit obtained from Pierce Biotechnology (Rockford, IL) was used according to the manufacturer's instruction. All other chemicals were of analytical grade. Human prostate carcinoma PC-3 cell line was obtained from Korea Cell Line Bank (Seoul, Korea). Green fluorescence protein (GFP) siRNA and GFP siRNA modified with a hexylamine group at 3′-end of its sense strand were purchased from QIAGEN (Valencia, CA). GFP siRNA modified at 5′-end of its sense strand with an indocarbocyanine dye (Cy3) was obtained from Dharmacon Research (Lafayette, CO).

2.2. Synthesis of amine-functionalized gold nanoparticles

Amine-functionalized gold nanoparticles were prepared by chemical reduction of gold precursor anions in the presence of cysteamine hydrochloride with slight modifications (Niidome et al., 2004). In brief, cysteamine hydrochloride (9.6 mg, 84.5 μmol) dissolved in 400 μL of deionized water was added to 40 mL of 1.4 mM $HAuCl_4$ solution in a 50-mL flask equipped with a stirrer. After stirring for 20 min, 1 mL of 1 mM $NaBH_4$ solution was added in a dropwise manner for over 2 min, and the mixture was stirred for 12 h. The resultant solution was purified by dialysis against deionized water in a Spectra/Por dialysis membrane with an MW cutoff of 10 kDa. For surface zeta potential studies, bare gold nanoparticles with an average diameter of 14.7 ± 1.5 nm were prepared by using a conventional citrate reduction method (Storhoff et al., 1998).

2.3. Synthesis of PEG-conjugated siRNA (siRNA–PEG)

The sequences of GFP siRNA were 5′-AACUUCAGGGUCAGCUUGC-3′ (sense) and 5′-GCAAGCUGACCCUGAAGUU-3′ (antisense). For confocal microscopy, Cy3-labeled siRNA was used. siRNA–PEG conjugate was synthesized by reacting

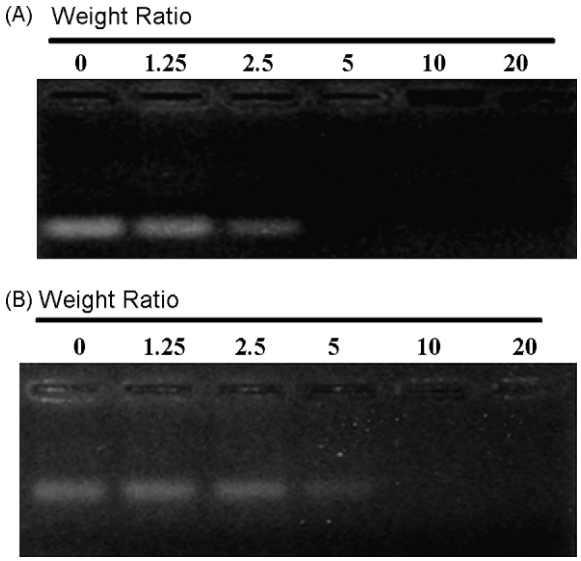

Fig. 1. Agarose gel electrophoresis of (A) AF-AuNPs/siRNA polyelectrolyte complexes and (B) AF-AuNPs/siRNA–PEG polyelectrolyte complexes.

mPEG–SH to 3′-hexylamine modified siRNA via a reducible disulfide bond as reported previously (Kim et al., 2006; Lee et al., 2007).

2.4. siRNA binding abilities of amine-functionalized gold nanoparticles

Amine-functionalized gold nanoparticles were mixed with 1 μg (10 pmol) of siRNA or siRNA–PEG conjugate at various weight ratios of gold nanoparticles to siRNA (0, 1.25, 2.5, 5, 10, and 20). After 15 min incubation, electrophoretic mobility of the mixture was visualized on a 2% (w/v) agarose gel. It was carried out for 25 min at 100 V in TAE buffer solution (40 mM Tris–HCl, 1% (v/v) acetic acid, 1 mM EDTA), and the band was stained with ethidium bromide.

2.5. Characterization of polyelectrolyte complexes of amine-functionalized gold nanoparticles with siRNA or siRNA–PEG conjugate

The polyelectrolyte complexes were prepared by mixing amine-functionalized gold nanoparticles with 1 μg of siRNA or siRNA–PEG conjugate at a weight ratio of 20 in deionized water, and then incubating for 15 min at room temperature. The hydrodynamic diameters were evaluated by using a dynamic light scattering instrument (Zeta-Plus, Brookhaven, NY). The measurement was carried out in triplicate. Size distribution and internal structure of the polyelectrolyte complexes were examined by TEM. Thirty microliter of the complex solution was deposited onto a 300-mesh carbon-coated copper grid, and then observed by a Zeiss Omega 912 transmission electron microscope (Carl Zeiss, Germany). To investigate the formation and dispersion stability of the polyelectrolyte

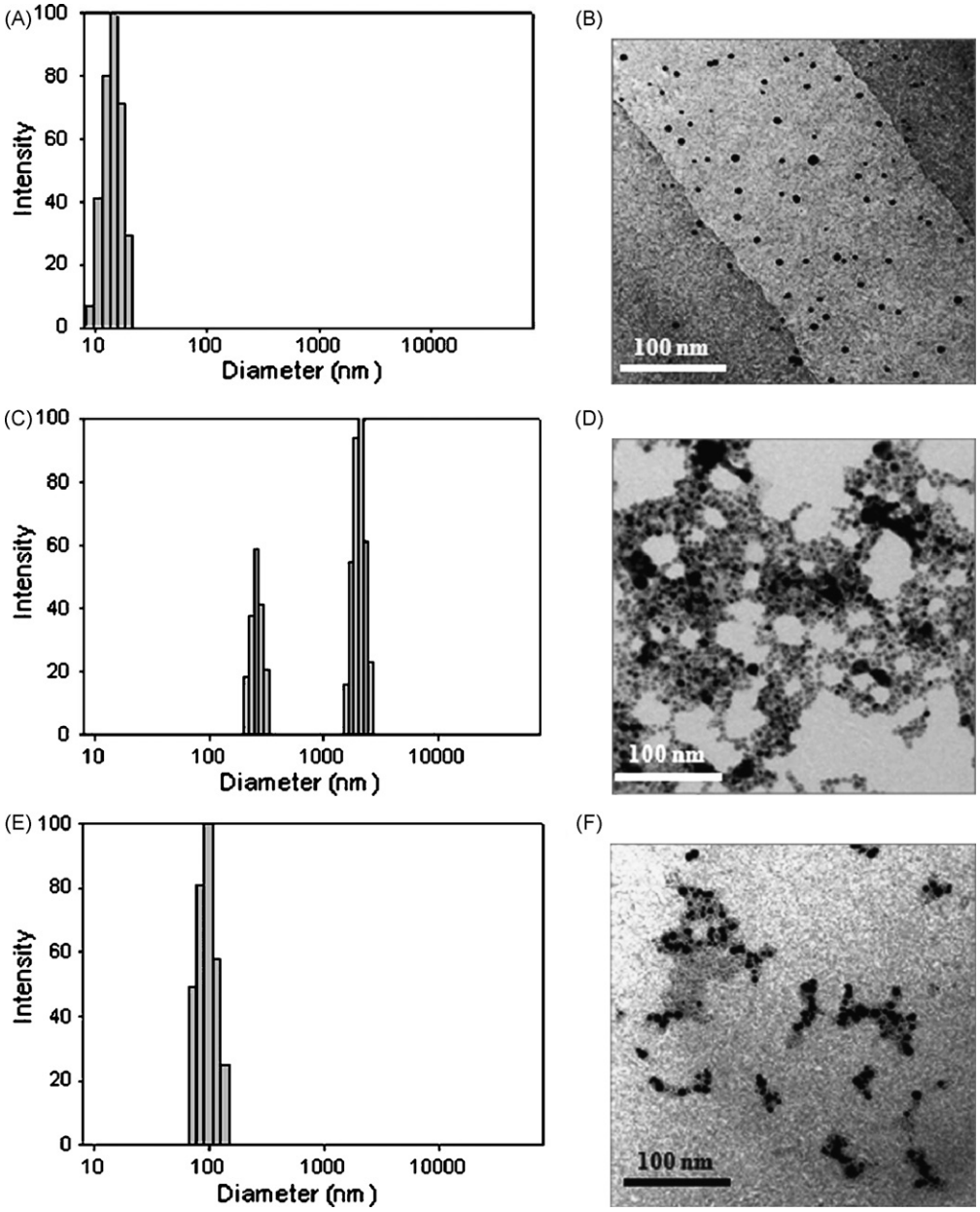

Fig. 2. (Left panel) Hydrodynamic diameters (A, C, and E) and (right panel) TEM images of (B, D, and F) for AF-AuNPs, AF-AuNPs/siRNA polyelectrolyte complexes, and AF-AuNPs/siRNA–PEG polyelectrolyte complexes.

complexes, UV–vis spectra were measured on a Shimadzu UV1601 spectrophotometer.

2.6. Evaluation of intracellular uptake and GFP gene inhibition effect of the polyelectrolyte complexes

Cy3-labeled siRNA or siRNA–PEG conjugate was used to prepare fluorescent polyelectrolyte complexes, in order to visualize their extent of intracellular uptake. PC-3 cells were plated on a chamber slide at a density of 1.5×10^5 cells per well and cultivated for 24 h at 37 °C. The cells were incubated with polyelectrolyte complexes of amine-functionalized gold nanoparticles (AF-AuNPs)/Cy3-labeled siRNA or Cy3-labeled siRNA–PEG (20 nM of siRNA, WR = 20) in RPMI medium supplemented with 10% (v/v) fetal bovine serum for 1 h at 37 °C. After washing with PBS solution, the cells were incubated with 100 nM of LysoTracker-Green as an endosome indicator for 30 min in serum-free media. Then the cells were washed with PBS solution and fixed with 1% (w/v) formaldehyde solution. After DAPI staining as a nucleus indicator for 5 min, the cells were examined by using a LSM510 confocal laser scanning microscope (Carl Zeiss, Germany). To evaluate GFP gene silencing effect of the polyelectrolyte complexes, the GFP-expressing DNA plasmid was co-transfected to PC-3 cells. PC-3 cells were seeded in a six-well plate at a density of 1×10^6 cells per well and incubated for 24 h at 37 °C. Two micrograms of pEGFP-C1 was mixed with 12 μL of Lipofectamine2000™ reagent in serum-free RPMI media for 30 min. After washing with PBS solution, the cells were incubated with the polyelectrolyte complexes and Lipofectamine2000™/pEGFP-C1 mixture in serum-free RPMI media for 5 h at 37 °C. The cells were harvested after 1 day and washed with PBS solution, and then lysed with 1% (w/v) Triton X-100. GFP fluorescence was measured at 520 nm by using a spectrofluorophotometer. The amount of total protein in each cell lysate was measured with a Micro-BCA protein assay kit. The relative GFP expression level was determined by dividing the amount of expressed GFP with the total amount of cellular proteins.

2.7. Cytotoxicities of amine-functionalized gold nanoparticles, branched PEI, and their polyelectrolyte complexes with siRNA

PC-3 cells were seeded in a 96-well plate at a density of 1×10^4 cells per well and grown for 24 h at 37 °C. The cells were then incubated for 4 h in serum-free RPMI media containing amine-functionalized gold nanoparticles, branched PEI, and their polyelectrolyte complexes (WR = 20 and N/P ratio = 16, respectively) at concentrations of 2, 4, 8, 16, 32, 64, and 128 μg/mL, and cultured with serum-containing fresh media for 2 days. Cell viability was determined by the CCK-8 cell viability assay, which measures mitochondrial dehydrogenase activity inside the cells. Briefly, 10 μL of CCK-8 solution was added to 100 μL of RPMI media in each well of the plate. After incubating the plate for 1 h at 37 °C, the absorbance at 450 nm was measured using the Bio-Rad microplate reader.

2.8. Statistical analysis

Statistical analysis was performed using a standard Student's *t*-test with a minimum confidence level of 0.05 for significant statistical difference. All experiments were performed in triplicate.

3. Results and discussion

3.1. Synthesis of amine-functionalized gold nanoparticles

Amine-functionalized gold nanoparticles (AF-AuNPs) were synthesized through chemical reduction of gold precursor anions in the presence of cysteamine hydrochloride on addition of sodium borohydride. The color of the reaction mixture changed from pale brown to dark red, indicative of the formation of colloidal gold nanoparticles. Since thiol groups of cysteamine were chemisorbed onto the surface of *in situ* formed gold crystals, the surface of gold nanoparticles were modified with primary amine groups. The molar ratio of gold precursor anions to cysteamine was kept at 1:1.5 to optimally stabilize the gold nanopartcles in aqueous solution according to the previous report (Niidome et al., 2004). AF-AuNPs were characterized by measuring zeta potential values and evaluating the degree of surface modification with cysteamine molecules. Bare gold nanoparticles prepared by a conventional citrate reduction method had a zeta potential value of -32.3 ± 4.4 mV, which was consistent with the previous finding (Liu et al., 2007). In contrast, the zeta potential value of AF-AuNPs was $+35.7 \pm 8.1$ mV, suggesting that primary amine groups were successfully introduced on the surface. Elemental analysis of AF-AuNPs revealed that each particle contained 12.4 wt.% of cysteamine, indicating that a single gold nanoparticle had ca. 5365 primary amine groups. The results demonstrated that gold nanoparticles were sufficiently modified with primary amine groups, which could be complexed with negatively charged nucleic acids for efficient cellular uptake.

3.2. siRNA binding abilities of AF-AuNPs

As illustrated in Scheme 1, AF-AuNPs were tested to form polyelectrolyte complexes with negatively charged therapeutic agents such as siRNA or siRNA–PEG conjugate by electrostatic interactions between phosphate backbone in nucleotides and primary amine groups on the surface of gold nanoparticles. To investigate

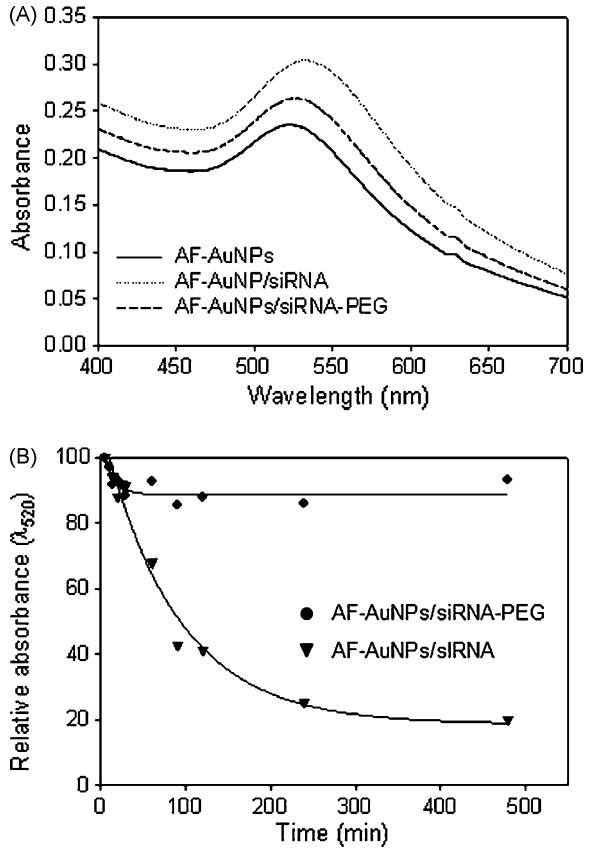

Fig. 3. (A) UV–vis spectra of AF-AuNPs, AF-AuNPs/siRNA polyelectrolyte complexes, and AF-AuNPs/siRNA–PEG polyelectrolyte complexes. (B) Time course change of absorbance value of the two polyelectrolyte complexes measured at 520 nm.

their siRNA binding abilities, AF-AuNPs were mixed with siRNA or siRNA–PEG at various weight ratios of gold nanoparticles to siRNA. After incubation for 15 min, electrophoretic mobility of the complex mixture was examined on an agarose gel by observing fluorescence of siRNA stained with ethidium bromide. As shown in Fig. 1, AF-AuNPs completely retarded the migration of siRNA at a weight ratio of 5. This implies that they could interact with siRNA via electrostatic interactions to form charge-neutralized polyelectrolyte complexes at that weight ratio (Sandhu et al., 2002). However, the electrophoretic migration of siRNA–PEG was completely inhibited upon addition of AF-AuNPs at a higher weight ratio of 10, suggesting that the conjugation of a neutral PEG chain adjacent to the siRNA segment could partially interfere with electrostatic interactions between negatively charged siRNA and positively charged gold nanoparticles, possibly due to the steric hindrance effect (Winblade et al., 2000; Mao et al., 2006; Jeong et al., 2007). Compared to PEI, as a standard carrier for siRNA, much higher weight ratio of AF-AuNPs/siRNA was required to completely retard the complexes than that of PEI/siRNA due to different charge density value between AF-AuNPs and PEI.

3.3. Characterization of polyelectrolyte complexes of AF-AuNPs with siRNA or siRNA–PEG conjugate

Dynamic light scattering (DLS) and TEM were employed to determine size distribution and internal structure of polyelectrolyte complexes of AF-AuNPs with siRNA or siRNA–PEG conjugate. As shown in Fig. 2A and B, AF-AuNPs were produced with a narrow size distribution of 14.4 ± 2.6 nm. When AF-AuNPs were mixed with siRNA, a binary mixture of heterogeneous aggregates was produced with an apparent average diameter of 260.5 ± 45.3 nm and 2.06 ± 0.38 μm after only 15 min incubation (Fig. 2C and D). In the TEM image, it can be clearly observed that gold nanoparticles shown as dark spots were significantly flocculated into a micron-sized three-dimensional architecture upon addition of siRNA. This was due to the uncontrollable aggregation of charge-neutralized polyelectrolyte complexes driven by siRNA-mediated crosslinking AF-AuNPs (Murthy et al., 2004). In contrast, AF-AuNPs/siRNA–PEG polyelectrolyte complexes had a well-dispersed nanostructure with an average hydrodynamic diameter of 96.3 ± 25.9 nm (Fig. 2E and F). Although they were not spherical, it can be visualized that around 10 gold nanoparticles on average are clustered to form ~100 nm sized nano-complexes. It has been shown in our previous studies that the siRNA–PEG conjugate undergo self-assembly into stable polyelectrolyte complex spherical micelles of ~100 nm by condensing with various core condensing polycations such as PEI and fusogenic KALA peptide (Kim et al., 2006; Lee et al., 2007). While a charge-neutralized inner core was spontaneously generated by ionic interactions between the negatively charged nucleotide segments and polycations, a hydrophilic and neutral PEG part is exposed outside to form a protective PEG shell layer. Thus, the surrounding PEG layer around the condensed AF-AuNPs/siRNA cores might play an important role in sterically preventing progressive aggregation, thereby leading to the ultimate stabilization of the AF-AuNPs/siRNA–PEG polyelectrolyte complexes in aqueous solution (Park et al., 2006; Kakizawa and Kataoka, 2002).

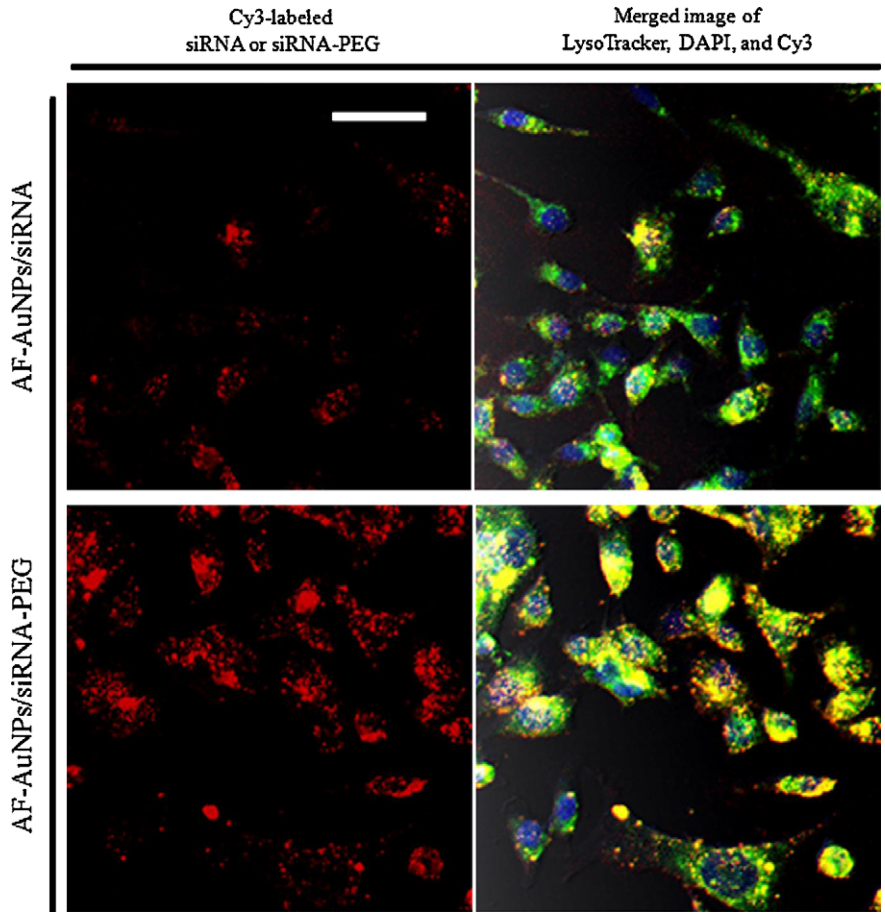

Fig. 4. Confocal microscopic images of PC-3 cells after incubating with AF-AuNPs/Cy3-labeled siRNA polyelectrolyte complexes (upper panel) and AF-AuNPs/Cy3-labeled siRNA–PEG polyelectrolyte complexes (bottom panel). Scale bar represents 50 μm.

To further investigate the stabilization effect of PEG chains on the formation of polyelectrolyte complexes, optical properties of AF-AuNPs were examined by UV–vis spectroscopy. The spatial arrangement of gold nanoparticles can be inferred by measuring the shift of a characteristic surface plasmon band that is influenced by their size, shape, aggregation state, and surrounding medium polarity (Daniel and Astruc, 2004). As shown in Fig. 3A, the surface plasmon band of AF-AuNPs appears prominently at 520 nm. However, the UV–vis spectrum of AF-AuNPs/siRNA polyelectrolyte complexes showed a broadening and dramatic red-shift of the surface plasmon band up to 545 nm. This can be attributed to the increased overlap of surface plasmon resonance from neighboring gold nanoparticles (Storhoff et al., 1998; Otsuka et al., 2001). The spectral change thus indicated that the interspatial distance between the gold nanoparticles significantly decreased as the nanoparticles were aggregated into a large three-dimensional cluster. However, the surface plasmon band of AF-AuNPs/siRNA–PEG polyelectrolyte complexes exhibited only a modest shift from 520 to 525 nm, suggesting that the gold nanoparticles complexed with the siRNA–PEG conjugate into a smaller cluster. The dispersion stability of these polyelectrolyte complexes was confirmed by time course change of absorbance at 520 nm (Fig. 3B). The absorbance value of AF-AuNPs/siRNA–PEG polyelectrolyte complexes remained even after 8 h, whereas that of AF-AuNPs/siRNA complexes decreased rapidly. The above results revealed that surface decoration of PEG chains around AF-AuNPs effectively protected the polyelectrolyte complexes from uncontrollable aggregation, thereby greatly enhancing their dispersion stability in aqueous solution.

3.4. Intracellular uptake and GFP gene inhibition effect of AF-AuNPs complexed with siRNA or siRNA–PEG conjugate

Intracellular uptake behaviors of AF-AuNPs complexed with siRNA and siRNA–PEG conjugate were examined by confocal laser scanning microscopy. PC-3 cells were used here as a model cancer cell line. Red color Cy3-labeled siRNA or siRNA–PEG conjugate was used to prepare polyelectrolyte complexes with AF-AuNPs, in order to visualize their sub-cellular distribution. Cell nuclei were stained with a blue color DAPI dye, and acidic endo-lysosomal compartments were stained with a green color Lyso-Tracker dye. Cy3-labeled siRNA and siRNA–PEG conjugate were taken up by the cells to a much smaller extent than their polyelectrolyte complexes with AF-AuNPs, because negatively charged nucleic acids were hardly interacted with the negatively charged cellular membrane, thereby limiting their cellular uptake (Kim et al., 2005) (data not shown). In contrast, AF-AuNPs/siRNA–PEG polyelectrolyte complexes were internalized more efficiently within cells than AF-AuNPs/siRNA ones in the serum containing media (Fig. 4). This result can be explained by the fact that the size of polyelectrolyte complexes is an utmost important factor in determining the extent of endocytosis and subsequent intracellular fate (Rejman et al., 2004; Chithrani and Chan, 2007). Since AF-AuNPs/siRNA polyelectrolyte complexes formed micron-sized aggregates, they would not be readily endocytosed by the cells. It is known that polymer nanoparticles less than ~200 nm are ideal for internalization within cells via an endocytic process. On the other hand, AF-AuNPs/siRNA–PEG polyelectrolyte complexes having an average diameter of around 100 nm exhibited more efficient cellular internalization than the AF-AuNPs/siRNA polyelectrolyte complexes. In the merged image, the cells treated with AF-AuNPs/siRNA–PEG showed much more intense yellow color, indicating that red colored Cy3-labeled siRNA–PEG was mostly co-localized with green colored endosomal vesicle compartments inside the cells. This suggests that most of AF-AuNPs/siRNA–PEG polyelectrolyte complexes were transported within cells via an endocytosis process

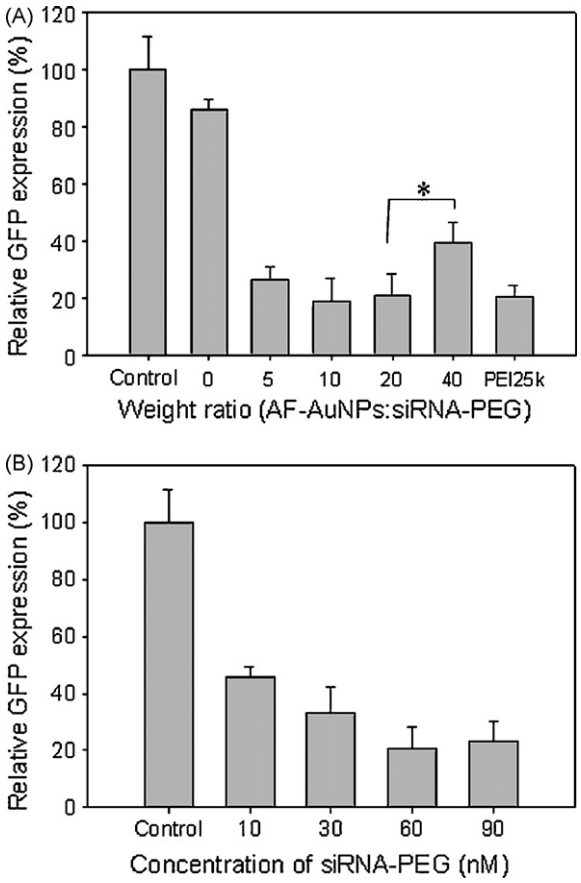

Fig. 5. (A) GFP gene silencing effect of AF-AuNPs/siRNA–PEG polyelectrolyte complexes as a function of the weight ratio of gold nanoparticles to siRNA–PEG conjugate. Branched PEI was used as a positive control at the N/P ratio of 16. The concentration of siRNA–PEG was 60 nM. * Statistically significant difference ($P < 0.05$) was observed at weight ratio between 20 and 40. (B) GFP gene silencing effect of AF-AuNPs/siRNA–PEG polyelectrolyte complexes depending on the concentration of siRNA–PEG conjugate. The weight ratio of gold nanoparticles to siRNA–PEG was 20.

and entrapped within the endosomal vesicles. The enhanced cellular uptake results agree well with the finding in Fig. 2 that siRNA–PEG conjugates adsorbed onto the surface of gold nanoparticles sterically stabilized the inner cargo of the charge-neutralized AuNPs/siRNA complex.

To investigate the GFP gene silencing effect of AF-AuNPs/siRNA–PEG polyelectrolyte complexes, the down-regulation degree of GFP in PC-3 cells was evaluated at various weight ratios of gold nanoparticles to siRNA–PEG. As shown in Fig. 5A, the extent of GFP expression efficiency after treatment of AF-AuNPs/siRNA–PEG was sharply reduced to $26.5 \pm 4.4\%$ at a weight ratio of 5. When the GFP expression level of non-treated cells was set as 100%, AF-AuNPs/siRNA–PEG polyelectrolyte complexes inhibited the GFP expression down to $20.7 \pm 7.5\%$ at the weight ratio of 20, whereas naked siRNA–PEG conjugate only suppressed down to $85.9 \pm 3.5\%$. With increasing the weight ratio from 5 to 20, the GFP gene silencing efficiencies maintained similar levels about 80% (no significant difference in a statistical *t*-test analysis), suggesting that the extents of cellular uptake for AF-AuNPs/siRNA–PEG polyelectrolyte complexes formulated at those weight ratios were not changed significantly. In contrast, the gene silencing efficiency was significantly reduced at the weight ratio of 40. This was probably because the increasing presence of cationic bare AF-AuNPs in the transfection media resulted in partly lowering the cellular uptake of AF-AuNPs/siRNA–PEG polyelectrolyte complexes by a com-

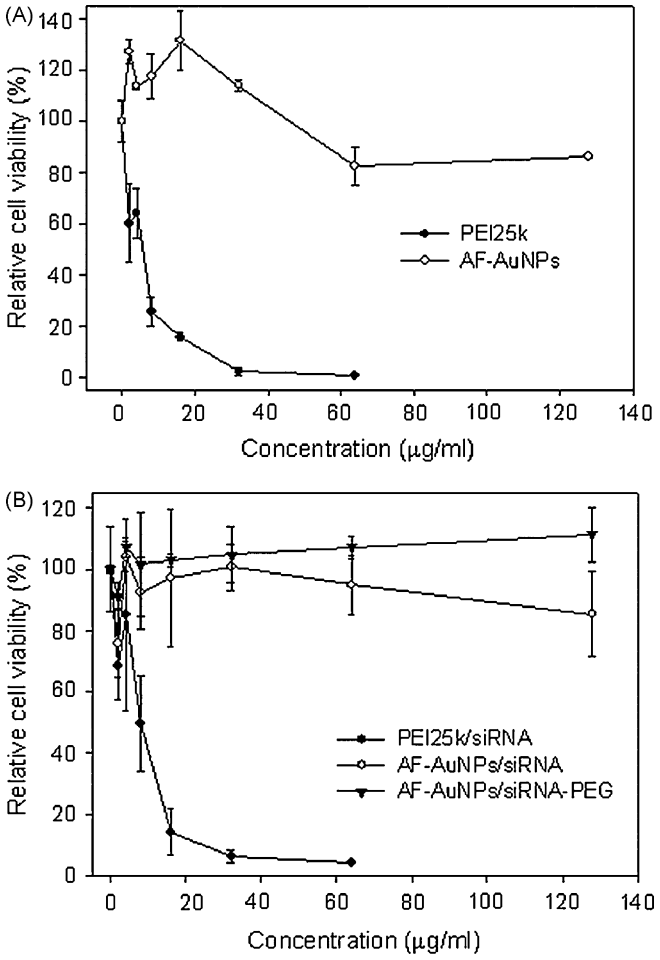

Fig. 6. Viability of PC-3 cells after incubating (A) AF-AuNPs and branched PEI and (B) their polyelectrolyte complexes with siRNA or siRNA–PEG conjugates at different concentrations.

petitive endocytosis process. Nonetheless, the far efficient gene silencing effect for AuNPs/siRNA–PEG polyelectrolyte complexes, as comparable as PEI/siRNA–PEG polyelectrolyte complexes used as a positive control, was clearly due to their colloidal stability and enhanced cellular uptake. Since siRNA and PEG in the conjugate was linked by a reducible di-sulfide linkage, an intact form of siRNA was likely to be regenerated within the cytosol by cleavage of the di-sulfide linkage under a reductive environment and proceeded to a series of RNAi events to degrade the target sequence of GFP mRNA (Kim et al., 2006; Lee et al., 2007). GFP expression was also suppressed in a dose-dependent manner (Fig. 5B). When the weight ratio was fixed at 20, the maximum inhibition of GFP expression could be attained at a concentration of 60 nM siRNA–PEG conjugate. Branched polyethylenimine (PEI) with an average molecular weight of 25,000 was used as a positive control because it was previously used as an effective carrier for the siRNA–PEG conjugate (Kim et al., 2006). Although the PEI/siRNA–PEG complexes significantly inhibited the GFP expression level down to $20.3 \pm 3.9\%$ at an N/P ratio of 16, it was found that branched PEI was much more cytotoxic than AF-AuNPs (Fig. 6A). As shown in Fig. 6B, branched PEI/siRNA polyelectrolyte complexes reduced the viability of PC-3 cells to $4.4 \pm 0.8\%$ at a concentration of 64 μg/mL, while AF-AuNPs/siRNA and AF-AuNPs/siRNA–PEG polyelectrolyte complexes induced only a marginal reduction in cell viability to $85.4 \pm 13.6\%$ and $111.5 \pm 8.8\%$, respectively even at a concentration of 128 μg/mL. Since the cytotoxicity was mainly caused by the presence of primary amine groups on the surface of AF-AuNPs, there was no large difference in cytotoxicity between AF-AuNPs/siRNA and AF-AuNPs/siRNA–PEG. It was reported previously that high-molecular weight PEI formed large clusters on the cell surface, which might impair biological functions of the cell membrane, finally leading to cell death (Thomas and Klibanov, 2003; Hunter, 2006). AF-AuNPs were relatively non-cytotoxic compared to PEI25k, which was probably caused from different amine densities. PEI charge density is fairly high as compared to AF-AuNPs. AF-AuNPs and PEI had about 1.6 and 5.7 nmoles of primary amines per gram carrier, respectively. The IC_{50} value of PEI25k was about 8 μg/mL, but that of AF-AuNPs could not be obtained because of no apparent cytotoxicity up to 128 μg/mL. Since gold nanoparticles have been shown to be non-immunogenic and non-cytotoxic (Shukla et al., 2005; Noh et al., 2007), AF-AuNPs are considered to be biocompatible gene carriers as evident from their low cytotoxicity. To validate our findings applicable in vivo administration, more detailed studies on AF-AuNPs/siRNA–PEG complexes such as stability in the presence of serum proteins, gene silencing efficiencies for different cell lines and primary cells, and further formulation optimization would be necessary.

4. Conclusions

The present study demonstrated the applicability of amine-functionalized gold nanoparticles for intracellular delivery of siRNA. These gold nanoparticles could interact with PEG-conjugated siRNA via electrostatic interactions to form nanosized polyelectrolyte complexes. The presence of PEG chains improved the dispersion stability of the polyelectrolyte complexes by protecting them from uncontrollable aggregation. The polyelectrolyte complexes of the gold nanoparticles with PEG-conjugated siRNA were much more internalized by human prostate carcinoma cells than the polyelectrolyte complexes prepared with siRNA alone. Furthermore, they efficiently suppressed GFP expression within the cells without eliciting severe cytotoxicity as compared with branched PEI. These novel gold nanoparticles would be potentially applied as a useful siRNA delivery system.

Acknowledgements

This research was supported by the Ministry of Health and Welfare and the National Research Laboratory program from the Ministry of Science and Technology.

References

Chithrani, B.D., Chan, W.C.W., 2007. Elucidating the mechanism of cellular uptake and removal of protein-coated gold nanoparticles of different sizes and shapes. Nano Lett. 7, 1542–1550.
Daniel, M.C., Astruc, D., 2004. Gold nanoparticles: assembly, supramolecular chemistry, quantum-size-related properties, and applications toward biology, catalysis, and nanotechnology. Chem. Rev. 104, 293–346.
Dorsett, Y., Tuschl, T., 2004. siRNAs: applications in functional genomics and potential as therapeutics. Nat. Rev. Drug Discov. 3, 318–329.
Dykxhoorn, D.M., Lieberman, J., 2005. The silent revolution: RNA interference as basic biology, research tool, and therapeutic. Annu. Rev. Med. 56, 401–423.
Hassani, Z., Lemkine, G.F., Erbacher, P., Palmier, K., Alfama, G., Giovannangeli, C., Behr, J.P., Demeneix, B.A., 2005. Lipid-mediated siRNA delivery down-regulates exogenous gene expression in the mouse brain at picomolar levels. J. Gene Med. 7, 198–207.
Hirsch, L.R., Stafford, R.J., Bankson, J.A., Sershen, S.R., Rivera, B., Price, R.E., Hazle, J.D., Halas, N.J., West, J.L., 2003. Nanoshell-mediated near-infrared thermal therapy of tumors under magnetic resonance guidance. Proc. Natl. Acad. Sci. U.S.A. 100, 13549–13554.
Hunter, A.C., 2006. Molecular hurdles in polyfectin design and mechanistic background to polycation induced cytotoxicity. Adv. Drug Deliv. Rev. 58, 1523–1531.
Jeong, J.H., Kim, S.W., Park, T.G., 2007. Molecular design of functional polymers for gene therapy. Prog. Polym. Sci. 32, 1239–1274.

Kakizawa, Y., Kataoka, K., 2002. Block copolymer micelles for delivery of gene and related compounds. Adv. Drug Deliv. Rev. 54, 203–222.
Kim, S.H., Jeong, J.H., Chun, K.W., Park, T.G., 2005. Target-specific cellular uptake of PLGA nanoparticles coated with poly(L-lysine)-poly(ethylene glycol)-folate conjugate. Langmuir 21, 8852–8857.
Kim, S.H., Jeong, J.H., Lee, S.H., Kim, S.W., Park, T.G., 2006. PEG conjugated VEGF siRNA for anti-angiogenic gene therapy. J. Control. Release 116, 123–129.
Lee, S.H., Kim, S.H., Park, T.G., 2007. Intracellular siRNA delivery system using polyelectrolyte complex micelles prepared from VEGF siRNA–PEG conjugate and cationic fusogenic peptide. Biochem. Biophys. Res. Commun. 357, 511–516.
Liu, Y., Shipton, M.K., Ryan, J., Kaufman, E.D., Franzen, S., Feldheim, D.L., 2007. Synthesis, stability, and cellular internalization of gold nanoparticles containing mixed peptide-poly(ethylene glycol) monolayers. Anal. Chem. 79, 2221–2229.
Mao, S., Neu, M., Germershaus, O., Merkel, O., Sitterberg, J., Bakowsky, U., Kissel, T., 2006. Influence of polyethylene glycol chain length on the physicochemical and biological properties of poly(ethylenimine)-graft-poly(ethylene glycol) block copolymer/siRNA polyplexes. Bioconjug. Chem. 17, 1209–1218.
Murthy, V.S., Cha, J.N., Stucky, G.D., Wong, M.S., 2004. Charge-driven flocculation of poly(L-lysine)-gold nanoparticle assemblies leading to hollow microspheres. J. Am. Chem. Soc. 126, 5292–5299.
Niidome, T., Nakashima, K., Takahashi, H., Niidome, Y., 2004. Preparation of primary amine-modified gold nanoparticles and their transfection ability into cultivated cells. Chem. Commun. 10, 1978–1979.
Noh, S.M., Kim, W.K., Kim, S.J., Kim, J.M., Baek, K.H., Oh, Y.K., 2007. Enhanced cellular delivery and transfection efficiency of plasmid DNA using positively charged biocompatible colloidal gold nanoparticles. Biochim. Biophys. Acta 1770, 747–752.
Novina, C.D., Sharp, P.A., 2004. The RNAi revolution. Nature 430, 161–164.
Otsuka, H., Akiyama, Y., Nagasaki, Y., Kataoka, K., 2001. Quantitative and reversible lectin-induced association of gold nanoparticles modified with α-lactosyl-ω-mercapto-poly(ethylene glycol). J. Am. Chem. Soc. 123, 8226–8230.
Park, T.G., Jeong, J.H., Kim, S.W., 2006. Current status of polymeric gene delivery systems. Adv. Drug Deliv. Rev. 58, 467–486.
Rejman, J., Oberle, V., Zuhorn, I.S., Hoekstra, D., 2004. Size-dependent internalization of particles via the pathways of clathrin- and caveolae-mediated endocytosis. Biochem. J. 377, 159–169.
Rosi, N.L., Giljohann, D.A., Thaxton, C.S., Lytton-Jean, A.K., Han, M.S., Mirkin, C.A., 2006. Oligonucleotide-modified gold nanoparticles for intracellular gene regulation. Science 312, 1027–1030.
Ryther, R.C.C., Flynt, A.S., Phillips, J.A., Patton, J.G., 2005. siRNA therapeutics: big potential from small RNAs. Gene Ther. 12, 5–11.
Sandhu, K.K., McIntosh, C.M., Simard, J.M., Smith, S.W., Rotello, V.M., 2002. Gold nanoparticle-mediated transfection of mammalian cells. Bioconjug. Chem. 13, 3–6.
Schiffelers, R.M., Ansari, A., Xu, J., Zhou, Q., Tang, Q., Storm, G., Molema, G., Lu, P.Y., Scaria, P.V., Woodle, M.C., 2004. Cancer siRNA therapy by tumor selective delivery with ligand-targeted sterically stabilized nanoparticle. Nucleic Acids Res. 32, e149.
Shukla, R., Bansal, V., Chaudhary, M., Basu, A., Bhonde, R.R., Sastry, M., 2005. Biocompatibility of gold nanoparticles and their endocytotic fate inside the cellular compartment: a microscopic overview. Langmuir 21, 10644–10654.
Storhoff, J.J., Elghanian, R., Mucic, R.C., Mirkin, C.A., Letsinger, R.L., 1998. One-pot colorimetric differentiation of polynucleotides with single base imperfections using gold nanoparticle probes. J. Am. Chem. Soc. 120, 1959–1964.
Thomas, M., Klibanov, A.M., 2003. Conjugation to gold nanoparticles enhances polyethylenimine's transfer of plasmid DNA into mammalian cells. Proc. Natl. Acad. Sci. U.S.A. 100, 9138–9143.
Winblade, N.D., Nikolic, I.D., Hoffman, A.S., Hubbell, J.A., 2000. Blocking adhesion to cell and tissue surfaces by the chemisorption of a poly-L-lysine-graft-(poly(ethylene glycol);phenylboronic acid) copolymer. Biomacromolecules 1, 523–533.